STRESS REDUCTION AROUND HOLES IN MECHANICALLY FASTENED JOINTS

Nashwan T. Younis, *Younis@engr.ipfw.edu* Professor of Mechanical Engineering, Indiana University-Purdue University Fort Wayne, USA

ABSTRACT

In this study, a different issue of mechanical engineering interests is determined for threaded fastened joints. A series of photoelastic experiments were performed to determine the maximum strains and the stress concentration factors (SCFs) for the holes in a tensile flat plate subjected to bolt-nut stresses. Pertinent strain distributions were examined to determine the roll of the torques on the bolts in minimizing the stress concentration. The experimental results indicate that SCF can decrease significantly with the increase of the bolt's pre-load.

Keywords: Stress intensity factor, Fastened joint

INTRODUCTION

The bolted joint is a type of mechanical connection which is used commonly for the construction of many types of structures. In fact, bolted joints are important in most of the mechanical devices and machines used in modern society. Also, it is becoming increasingly important to reduce the SCFs due to the presence of holes and other discontinuities in many design situations. As a result, many researchers have investigated the stress concentrations around holes in plates subjected to uniaxial tension [1]; the literature is bereft when describing the effect of mechanically fastened joints. Currently, the study of SCF around circular holes has reached a plateau. However, the quest for better, sophisticated, and stress relieved members continues almost exponentially. One method for reducing the stress concentration around a circular hole in a plate subjected to a uniaxial load is by introducing defense holes. A survey of the literature shows that this method has been the most studied. A number of techniques have been developed to reduce the stresses around holes. These include, for example, the analytical work of Tings, Chen, and Yang [2, 3]; the numerical contributions by Meguid [4], and the experimental contributions [5]. Recently, numerical and experimental studies have been conducted to investigate the effect of reinforcements around circular cutouts on the stress concentration and buckling behavior of carbon/epoxy composite panel under in-plane shear load [6]. In 2008, Liqing and Bingzheng [7] utilized the three dimensional finite element method to solve the problem of the quarter-elliptical corner crack of the bolt-hole in mechanical joints subjected to remote tension.

In regard to bolted joints, several authors have suggested both theoretical and experimental methods to determine member stiffness and the pressure distribution between the members of bolted joints. Grosse and Mitchell [8] gave a general discussion of non-linearities in bolted joints due to the application of external loads as well as bolt thread and interfacial friction. Member stiffnesses and the stress

distributions in the bolts and members of bolted joints have been calculated for various bolt sizes as well as thicknesses and materials of the members [9]. In 2000, Lehnhoff and Bunyard determined SCF for the threads and the bolt head fillet in a bolted connection [10]. They concluded that the results can provide important insight into the behavior of bolted connections. Barrett [11] shared his 34 years experience in fasteners and mechanical design by providing guidelines to reduce fastener's stress risers. Among his recommendations about threaded members, the threaded portion should have a minor diameter greater than the diameter of the unthreaded portion. This eliminates the SCF, as long as a generous transition radius is used between the two sections. In 2005 [12], the stress distribution in bolt-nut connectors was studied using an axisymmetric finite element model. The design modifications included grooves and steps on the bolt and nut, and reducing the shank diameter of the bolt. Turvey and Wang's [13] analysis showed that friction between the bolt shank and the hole as well as the small hole clearance are the principal factors which cause the zone of contact to increase with increasing tension; thus produce significant changes in the stress distributions at critical locations. The importance of the pre-tensioned force of bolts has been recognized by Gao and Kang in 2008 [14]. It was noted that the greater the force, the larger the region of stress redistribution around a roadway is affected.

Common type of connections used for structural works are welded, riveted, bolted, and pin connections. Pinned connections are used to connect the members which are required to rotate relative to each other. A study of the pin and the plate material dissimilarity was done by Iyer [15]. A fiber steering technique was applied around the hole in carbon fiber reinforced plastics laminated composites to increase the bearing strength [16]. Okutan [17] carried out a numerical and experimental study to determine the effects of geometric parameters on failure. In 2005 [18], a three dimensional progressive damage model was developed by McCarthy et al. to show the significant effect of clearance on load distribution and damage mechanisms in the joint. In order to have a good evaluation of the stress distribution around the pin's hole, design factors such as plate width, edge distance and clearance were varied during the analyses by Yavari et al. in 2009[19].

Problem Statement: The objective of this paper is to present the results of a study of the elastic field resulting from interacting circular holes with a bolt-fastener. The work aims at determining the SCF around holes interacting with bolts at different bolts preload. This topic represents an important design issue because the introduction of assembly stresses results in reduction of SCF at the holes. Therefore, in the present program, the reflected photoelasticity method is utilized to determine SCFs for tension of a plate with a circular hole displaced from the center by a distance L and approaching the fasteners as shown in Fig. 1. In this figure, (x, y) and (r, θ) are the rectangular and polar coordinates with the origin at the center of the plate. The most significant advantage of choosing

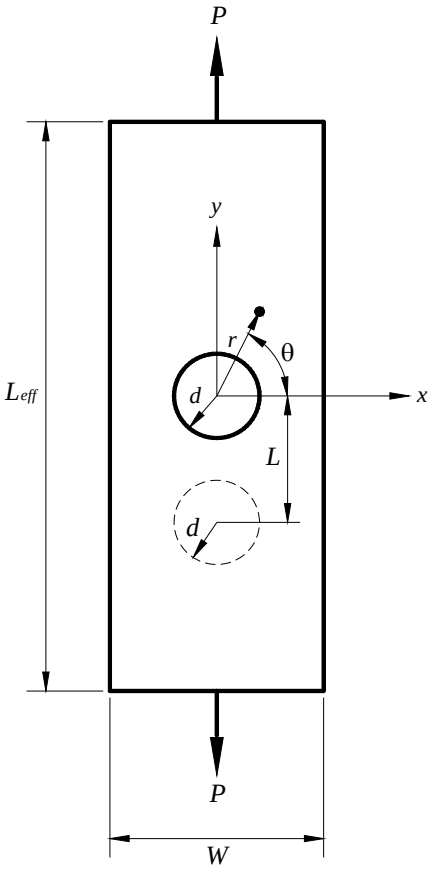

Figure 1. Specimen Parameters.

reflected photoelasticity, it is not necessary to model the realistic behavior of all elements involved in the study.

THEORY

Reflected photoelasticity is based on the optical phenomenon of birefringence and the fringe orders represent the difference in principal strains (maximum shear strain). The method is nondestructive and the coatings can be applied directly to the prototype. Thus, the need for models is eliminated. The basic relationship between the observed fringe order using normal-incident method, N_n, and the difference between the principal strains is [20]:

$$\varepsilon_1 - \varepsilon_2 = \gamma_{\max} = N_n f \qquad (1)$$

The principal strains are the ones in the coating and metal surface. The fringe value f specifies the strain-optic sensitivity of the coating taking into account the thickness of the coating, the nature of the light source and the fact that the light transverses the coating twice. Engineers often work with stress rather than strain. Members' stresses in situations using threaded fasteners are primarily caused by three different modes: tensile of a member, compressive bearing of the bolts on a member, and contact

stresses. The elastic principal stresses in the structure can be calculated using the generalized Hooke's law as:

$$\sigma_1 - \sigma_2 = \frac{E}{1+\nu}(\varepsilon_1 - \varepsilon_2) \qquad (2)$$

Where E is Young's modulus and ν is Poisson's ratio. Substituting equation (2) into (1), the difference of principal stresses in the part becomes:

$$\sigma_1 - \sigma_2 = N_n fE/(1+\nu) \qquad (3)$$

A thick coating of thickness t produces a reinforcing effect that must be taken into account. This is because when the test specimen is thin, the coating may carry an appreciable portion of the loading. Thus, a correction must be made to account for the changes in thickness and material. Considering the forces on coated and uncoated elements, one can obtain the theoretical correction factor as:

$$C = (1 + \frac{t_c E_c (1+\nu_s)}{t_s E_s (1+\nu_c)} \qquad (4)$$

The subscript c is for the coating and subscript s is for the specimen. When readings are made at free boundaries, such as circular holes in this study, the calculated stress represents the stress tangent to the free surface because the stress perpendicular to the edge is known to be zero. Thus, the maximum corrective stress at the hole's boundary is:

$$\sigma_{max} = CN_n fE/(1+\nu) \qquad (5)$$

The nominal stress in the plate of width W at the net cross-sectional area is:

$$\sigma_{nom} = \frac{p}{(W-d)t} \qquad (6)$$

P is the applied load and d is the diameter of the hole. Thus, the stress concentration factor is:

$$K = \frac{\sigma_{max}}{\sigma_{nom}} \qquad (7)$$

If the coating thickness is constant and using equations (5)-(7), the stress concentration factor becomes:

$$K = \frac{CN_n ftE(W-d)}{P(1+\nu)} \qquad (8)$$

Equation (8) represents the basic relationship underlying the determination of the stress concentration factors at the edge of circular hole.

DESIGN OF EXPERIMENT

In this section, important elements of the experimental design are outlined through discussion of the method of measurement, the uncertainty in expected results, and the choice of specimens. The experiment design protocol used was as outlined by Holman [21]. The type of experiment is testing according to accepted method because there are accepted procedures for determining SCF utilizing

optical methods. The method of photoelasticity was used because it inherently provides information in the vicinity of stress raisers as well as it is a full-field solution for stress analysis testing. The photoelastic fringe pattern is also rich with information and insights for the design engineer. The method allows testing of the actual product or structure under actual working loads at room temperature. In this study, the method was chosen so that the effects of fastened joint on SCF can be determined without assumptions.

The measured quantities needed to calculate SCF were: mechanical properties of the material, specimen's dimensions, and photoelastic parameters. The determination of the properties (modulus of elasticity and Poisson's ratio) and the measurement of the dimensions (width, thickness, and hole diameter) can be achieved easily with very high accuracy. Uncertainty in the anticipated fringe patterns and values necessitated the determination of an estimate of the range of the stresses around the hole. This was essential in selecting the photoelastic coating. Assuming a linear stress field resulting from the joint stress σ_j, the initial estimate of the maximum stress σ_{max} was calculated as:

$$\sigma_{max} = \sigma_{w/o} - \sigma_{j.} \qquad (9)$$

$\sigma_{w/o}$ is the stress at the hole neglecting the joint effect. The joint stress was estimated from:

$$\sigma_j = \sigma_b + \sigma_c \qquad (10)$$

σ_b and σ_c are the bearing and contact stresses, respectively. The above calculations indicated that a medium-high sensitivity coating of a thickness range 2.8-3.3 mm was needed. The preliminary calculations of the bolt's stress and contact stress between the fastener joints and the test plates resulted in the design of the testing plate with the dimensions shown in Fig.2. The uncertainty in the interaction between the different stress fields led to initially design the bolts arrangements in a single row. Initial fringe patterns indicated that bending of the plate could happen. Thus, the arrangement of the bolts was modified to the one shown in Fig. 2.

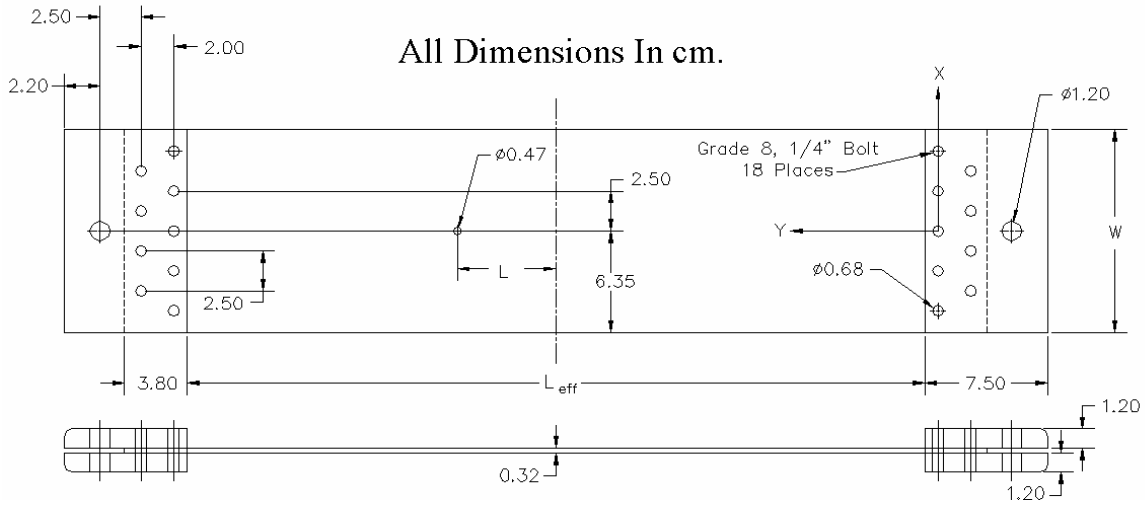

Figure 2. Detailed Geometry of Bolted Connection

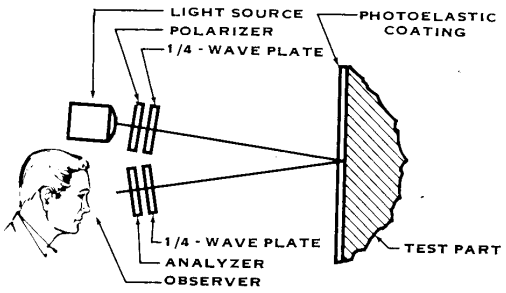

Figure 3. Schematic Experimental Setup

EXPERIMENTAL SETUP

In the photostress method, strain measurements are made by reflecting polarized light from the surface of a stressed part to which a photoelastic coating is being applied. A reflection polariscope is used to observe and measure the surface strains. The coating is a thin sheet of birefringent material, usually polymer. Starting with the unload test part, and applying the loads in increments, fringes will appear first in the vicinity of the hole. As the load is increased, new fringes appear near the joint. With further loading, additional fringes are generated in the highly stressed regions and move toward regions of less stress.

A typical commercial reflection polariscope consists of mounted polarizer and quarter-wave plate attached to the common frame. They are mechanically connected so that they rotate in unison. The instrument may be hand-held or mounted on a tripod. The schematic for the optical system is shown in figure 3.

TEST SPECIMENS DETAILS

Many aluminum specimens with different lengths, widths, and hole locations were considered in this investigation. Two sets of specimens, each consisting of ten plates, were studied. The effective length (L_{eff}), width, and thickness of the machined specimens for the first set (S_{one}) were 49.6 cm, 12.8 cm, and 0.32 cm respectively. There was a 0.47 cm diameter hole bored through each plate at different locations. The effect of the edges on the stresses around the hole was kept small by holding the ratio of d/W to less than 0.0375. For the second set (S_{two}), the plates were 34.2 cm long, 11.43 cm wide and 0.32 cm thick and the hole diameter was 0.32 cm. Nine SAE grade eight type bolts and nuts on each end were used. The torque on all the screws was kept the same at each applied torque. After the plate's surface was prepared, a 3.0 ± 0.05 mm thick PS-1A photoelastic sheet was bonded to the surface of the plate. The combination of the thickness and the type of coating chosen was to obtain a low fringe value or more sensitive coating.

Two specimens from each set were coated entirely and the remaining eight were coated approximately 60- 75% of the free surface. This allowed the use of the same sheet of photoelastic material, hence

reducing the variables in the experiments. When the test part extended beyond the edge of the photoelastic coating, the edges were beveled at 45 degrees to eliminate any undesired stress concentrations at the edges. The coating must match and be perpendicular to the boundary of the plate; especially it is important around any discontinuity. Therefore, the holes were drilled through the coating and the plate. The author's experience indicates that this procedure provides better matching of the edges of the coating and the boundary of the test part at the hole than to precut a hole in the plastic before bonding. The absence of residual birefringence supports the simple proposed technique.

DISCUSSION OF THE RESULTS

Testing procedures were performed to evaluate the significance of the parameters influencing the data and to facilitate an engineering assessment of the results obtained. Instrumentation systems have in common an intrinsic characteristic which inevitably limits their accuracy in varying ways and degrees, and reflected photoelasticity is not an exception. This characteristic is the tendency to respond to other variables in the environment in addition to the variable under investigation. Since many variables contribute to the stresses around the hole in this study, the effect of the ratio of the hole size to the plate's width is beyond the scope of this paper. However, to significantly reduce the interaction between the plate's width and the hole's size, the ratio d/W was chosen based on the recommendation of reference [22].

Strain Field: Utilizing the photoelastic images, the development of Saint-Venant's stress region was presented in 2010 [23]. Therefore, the photoelastic coating was marked with a point every 5 mm horizontally and vertically close to the joint and 10 to 20 mm away from the threaded joint. The plates without holes were subjected to axial tensile loads while the bolt's preload was kept constant, finger tied. During the difference in principal strains (maximum shear strain) acquisition, the fringe patterns were studied to identify the effects of the fasteners and fastener joints. Approximately, symmetry of the fringe patterns about the vertical centerline of the specimens and the horizontal centerline was noticed utilizing the entirely coated two plates.

Next, the bolt's preload was varied. It is not practical to give a detailed strain distribution for each load in this paper, but the results in Fig. 4 of S_{one} plates are presented as a typical example. The maximum shear strain is for a tensile load of 22,000 N and the torque on each bolt is 6.8 N.m. Theoretically, for a plate loaded in tension, the stress over the entire plate should be uniform. It is clear that the strains close to the plate's center are constant and in agreement with the theoretical ones. However, the difference in principal strains (hence the stresses) varies rapidly in the vicinity of the threaded joint. This deviation is due to the bolted fasteners. Interestingly, the plate's stresses near the center bolt are approximately zero. This low stress zone will house part of the holes in four specimens. Bearing stresses are developed on surfaces of contact where the shank or threaded parts of

bolts are pressed against the sides of the hole through which they press. Since the distribution of theses forces for even a single bolt is complicated, an average bearing stress is often used in the literature for design purposes. This stress is usually computed by dividing the force transmitted across the surface of contact by the projected area $A = d_b\ t$ where d_b is the bolt diameter. Clearly, figure 4 shows that the customary assumption that the bearing stresses are uniformly distributed is not accurate. It was noted during the strain development acquisition phase that the fasteners and fastener joints affect S_{two} plates more than that of the S_{one}. This is because S_{two} plates are shorter, thus less material to absorb the bearing and contact forces.

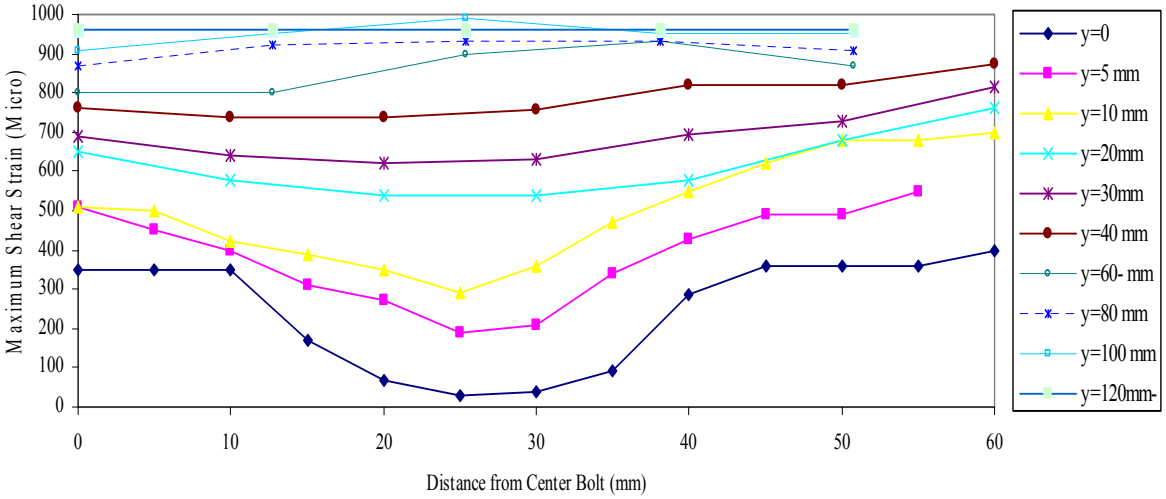

Figure 4. Strain in the plate without Hole

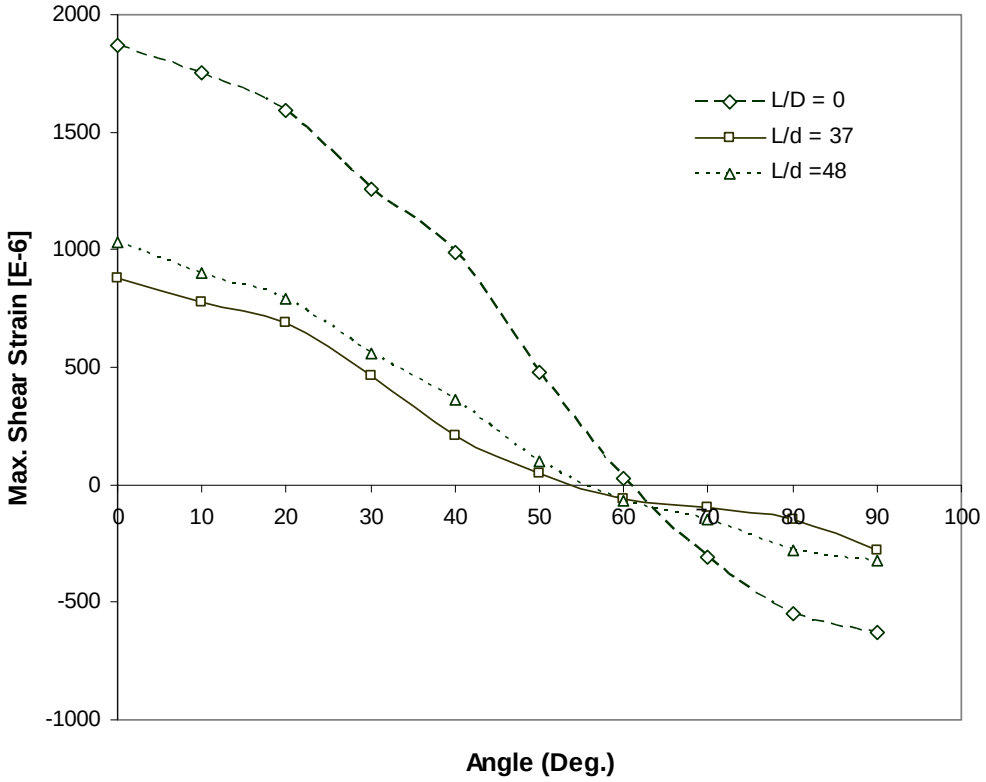

Figure 5. Distribution of Strain along Hole Circumference

Effect of Hole's Location: Holes were bored at different locations and the distribution of the tangential strain about the boundary of the holes was studied. Each specimen was incrementally loaded at various levels with the maximum stress being kept below the yield strength. The torque was varied from 0 to 8.5 N.m in the experiments. In general, it was noticed that the strain distribution is linear and increases as the hole approaches the center except for the lowest applied load of 4500 N. This deviation was attributed to the fact that the deformation was very small and the coating's sensitivity is low at this stress level. The variations of peak strains with the loads showed the same general trends in the specimens. The effect of the geometric parameter (L/d) on the maximum shear strain around the hole is shown in figure 5. This distribution is for S_{one} specimens with a load of 14500 N and a torque of 2.7 N.m. It is clear that both the maximum tensile and compressive strains decreased as the hole was off-center. However, the strain increased as the hole approached the edge of the plate where it was held by the bolted fastener but still below the ones associated with the holes close to the center. This was due to the fact that the area between the edges of the hole and bolted plates was very small; to increase the stress at the same time, the other plates increase the stiffness, which reduces the stresses. Next, strain analysis in the vicinity of the holes for the S_{one} specimens was performed. Generally, the trends of the results are the same for both groups. The results indicate that it is advantageous to use the compressive nature of the bolted joints to reduce the strain (stress) around a circular hole.

Effect of Torque: Bolt-nut connectors play an important role in the safety and reliability of structural systems. In this section, the torque in bolt-nut connectors is studied to determine the extent to which it reduces stress concentrations. Figures 6-8 are examples of how the maximum shear strain varies as a function of the bolt's torque in S_{two} specimens. It is noted that the torque effect is minimal when the hole is away from the bolts. Figure 6 shows the effect of various torques on the maximum strain around the hole for L/d=30 in which the strain decreases with increasing torque up to T = 4.3 N.m. The effect of higher torque can be observed as L/d increases to 35 as shown in figure 7. It can be seen that the strain consistently decreases with an increase of the torque. This demonstrates that higher torquesincrease the compressive bearing stress which is in the same direction as the applied load. This analysis takes into account the bolt-hole clearance as well as the friction at the contact surfaces between the bolt shank and the inserting hole. This friction is the principal factor that causes the zone of the bearing area distribution.

Regarding the strain dependence on higher torque, it was observed that the effect of T = 8.5 N.m became apparent as L/d increased. Figure 7 illustrates the effect of torques on strain as the hole approaches the joint, L/d = 42.5. Although the strain continues to decrease, the difference between the previous torques significantly diminished as the strains are so nearly the same that they are overlapped.

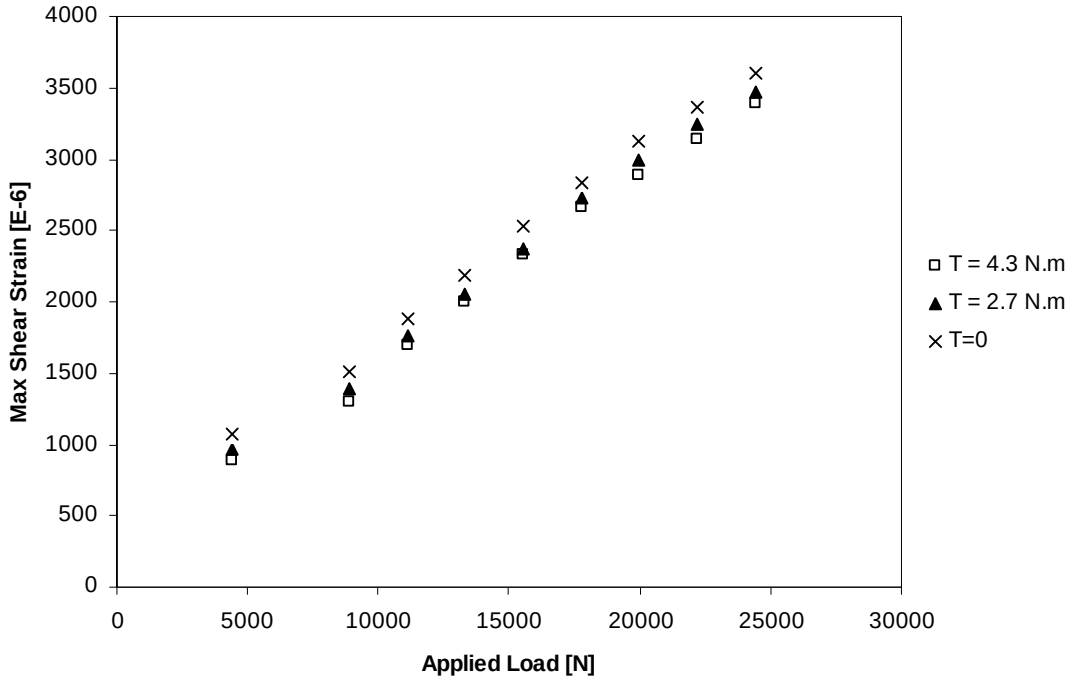

Figure 6. Effect of Torque on Strain for L/d=30

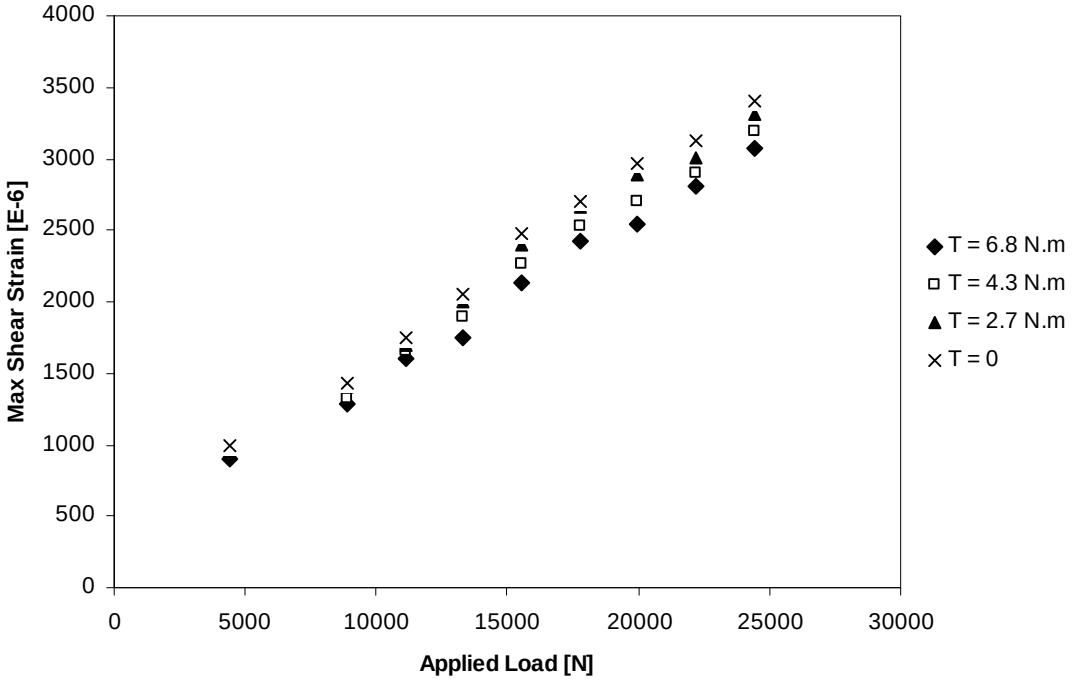

Figure 7. Effect of Torque on Strain for L/d=35

Furthermore, the influence of the contact stress on the results is significant. It can be found from Fig.8, L/d = 50, the effect of the compressive stress on the fastener joints has introduced the three-dimensional stress as evident by changing the trend of the maximum shear strain. The strain increases as a result of both the hole approaching the fastener and the increase in torque. Figure 9 is a design chart relating hole location and pre-load to percentage reduction on strain. The maximum strain at the edge of the central hole is considered to be the reference value.

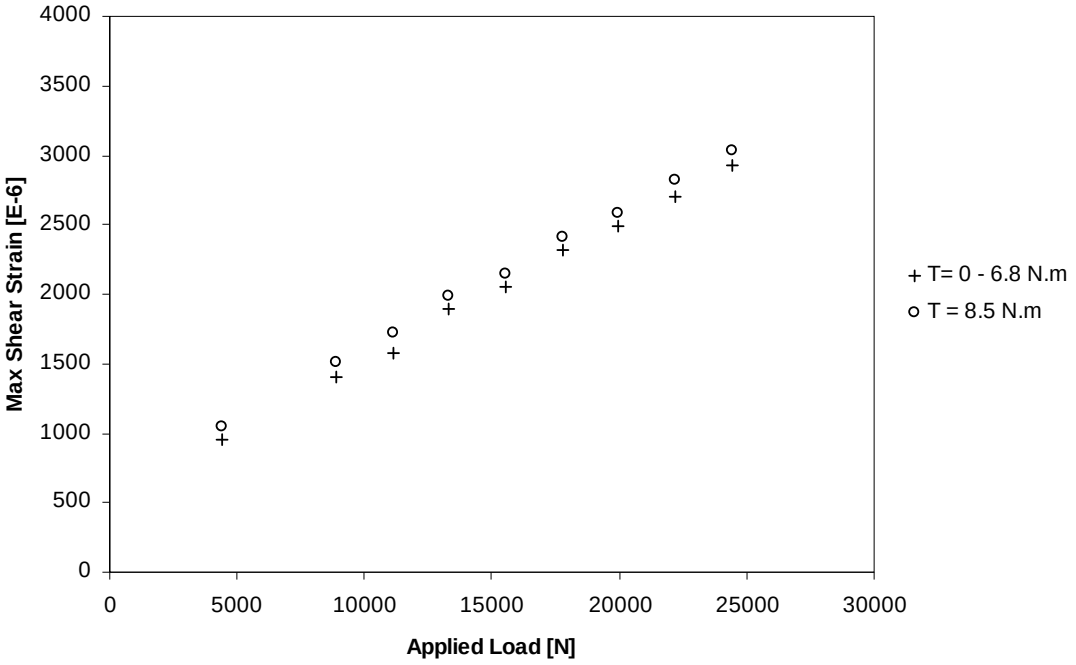

Figure 8. Effect of Torque on Strain for L/d=42.5

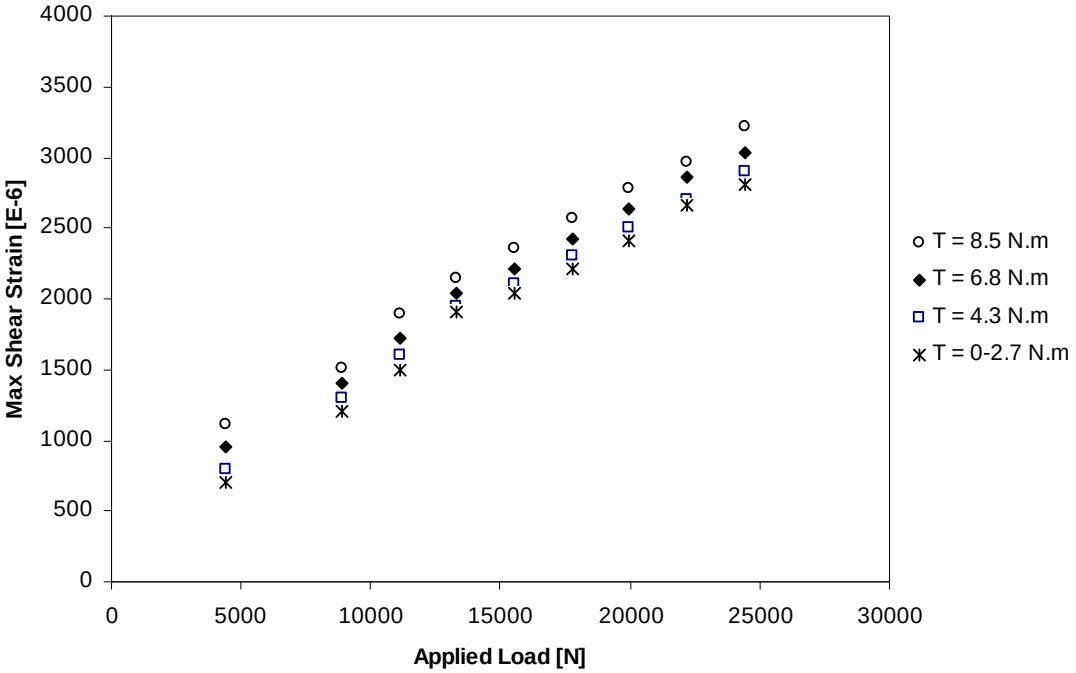

Figure 9. Strain Distribution Very Close to the Fastener (L/d=50)

Stress Concentration Factor: One of the objectives of application accurate SCFs is to achieve better-balanced designs of structures and machines. Therefore, conserving material, obtaining cost reduction, and achieving lighter and more efficient apparatus. Since a detailed strain results for S_{two} plates are presented in the previous section, the results of S_{one} plates will be summarized here. The SCF value is plotted in figure 10 as a function the distance center-to-hole diameter ratio, L/d. It is important to remember that the ratio of the hole diameter-to-the width of the plate was constant. Interaction

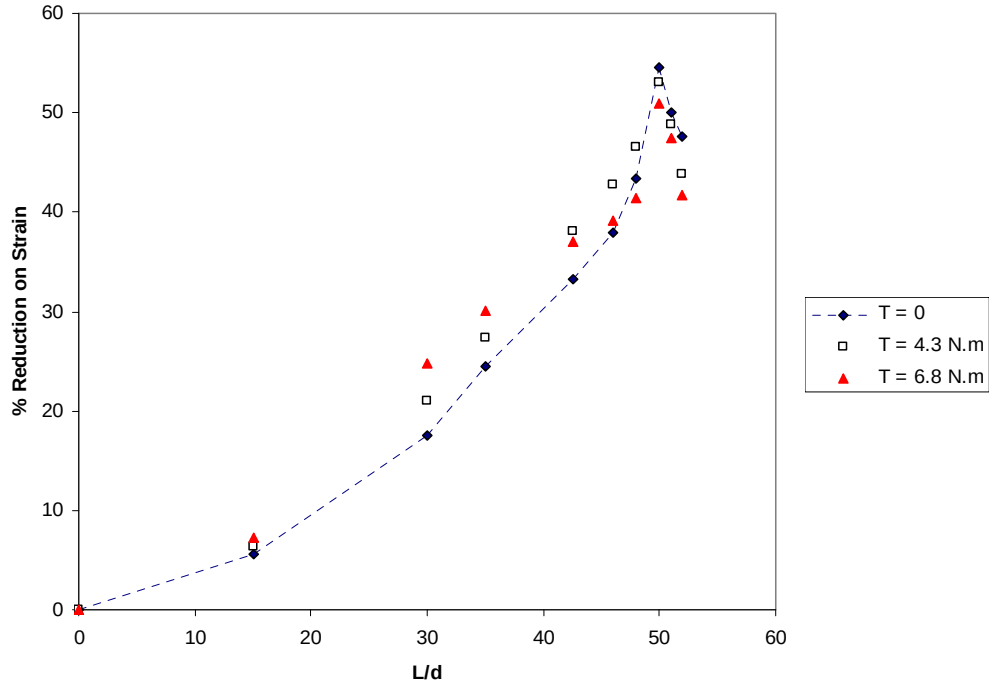

Figure 10. Design Chart Showing Percentage of Reduction in Strain

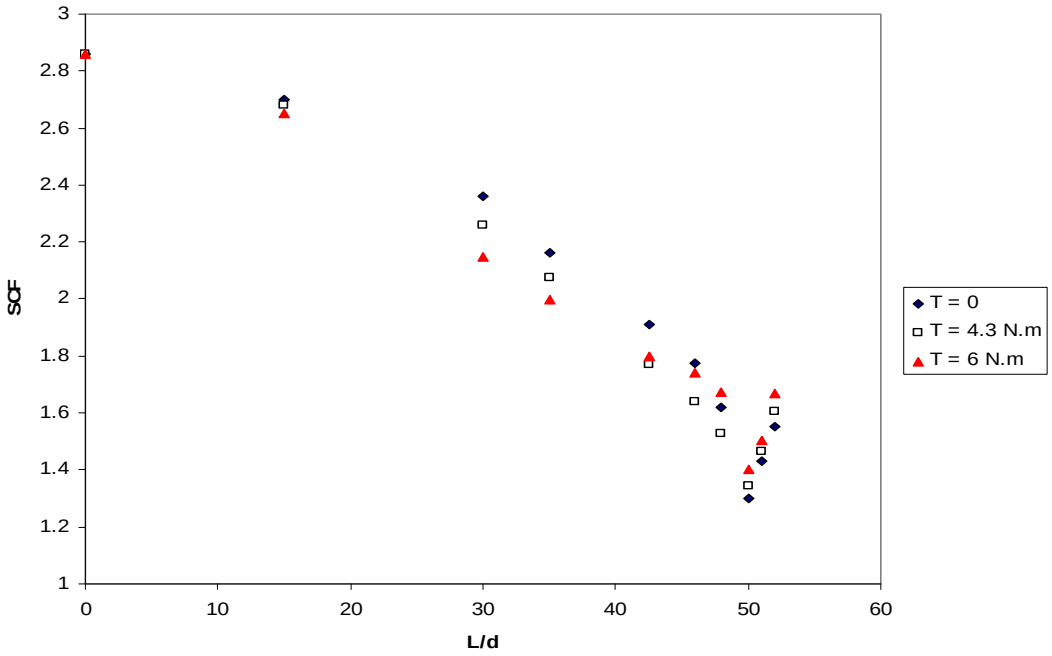

Figure 11. Effects of Location and Torque on SCF

between the different stress fields could result in some advantages and disadvantages regarding the stresses in different regions. It is evident from figures that the SCF around the hole decreased as the hole moved toward the fastened joint, but increased as the hole approached the edge of the plate where it was held by the threaded fixture. At the center of the plate, only the applied tensile axial stress σ_a is affecting the stresses around the hole as identified in Fig. 12a. The SCF decreased as the hole was off-center due to the presence of the compressive bearing stress that is superimposed the axial stress as

illustrated in Fig. 12b. As an example, for a torque of 4.3 N.m, the SCF affected by the bearing stress (L/d= 48) is 53% less than that of the central hole.

It can be found from figure 10 that the SCF increased when the hole is very close to the bolts. Furthermore, it can be observed that SCF exhibit a phenomenon of sharp increase with the addition of torque. These increases are attributed to the tearout shear stress τ as well as the contact stress on the fastener joints due to the preload of the bolts (see Fig. 12c). The addition of the shear stress increases the in-plane principal stress which results in increasing the SCF. The bolts' preload induces a contact stress that is perpendicular to the surface of the plate. Due to the Poisson's ratio effect, σ_c increases the in-plane principal stress and hence the SCF. For the same above torque T= 4.3 N.m, the SCF increases by 20% (L/d = 50 and 52), but the higher stress is 32% less than that of the central hole.

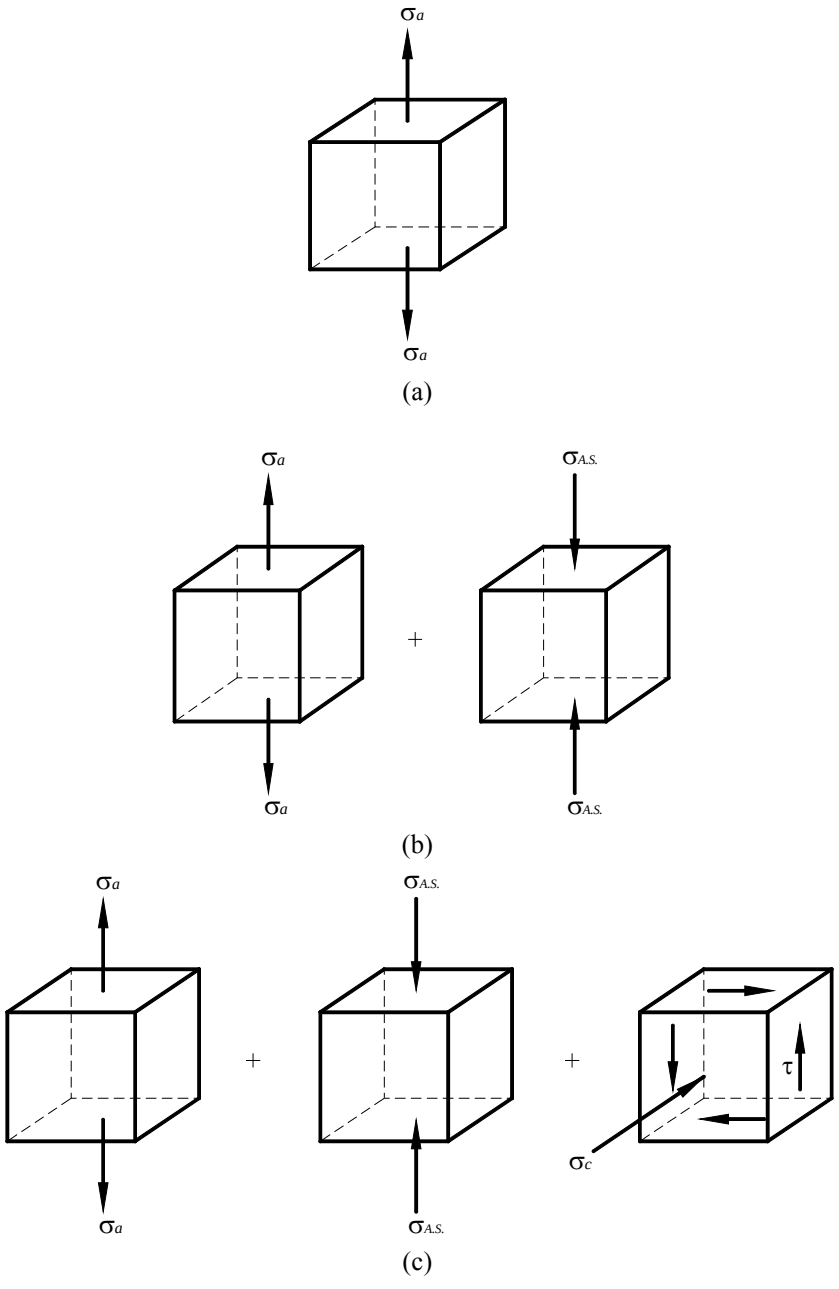

Figure 12. Interaction between Stresses

CONCLUSIONS

The reflected photoelasticity method is utilized to study the reduction of stresses in a mechanically fastened joint. The complication of realistic deformation modeling is eliminated because the coatings can be applied directly to the prototype. Several specimens are manufactured to predict the strain near a hole at different locations. The study takes into account the preload on the fasteners and fastener joints. All stresses (axial, bearing, contact, and bolts) aspects are investigated for each specimen to show how these stresses interact in rather complicated manner. The following observations have been made in the course of conducting this study:

1. The strain increases almost linearly and smoothly as the load increases for each specimen even when the torque exceeds the recommended preload for reused connection. An engineer must decide on the advantage of a preload in reducing SCF around a hole and the fatigue life of the bolt.
2. At a fixed bolt's preload, the SCF decreases as the hole approaches the fastened joint which could increase the fatigue life of a member. SCF increases when L/d is greater than 50 but it is still below that of the holes near the center of the plate.
3. The influence of the bolt's torque is significant in the resulting strain. Low torques imply greater strain in the region where L/d is between 30 and 40. However, larger torques increases strain (hence SCF) in the close proximity of a mechanical fastened joint. In spite of this increase, SCF is still below the ones close to the center of the plate.
4. The interaction between axial, bearing, bolts, and contact stresses is dependent on the hole's location.
5. Friction between the bolt shank and the hole is the principal factor which causes the zone of contact that affect the strain around a hole in the plate.
6. Drilling a hole near a fastener is a practical solution in reducing stresses around holes. A combination of a hole location and a bolt preload can reduce the SCF by more than 50%. The results provide insight into reducing SCF as a result of threaded assembly stresses.

Finally, the results of this research should be applicable to many plate design problems where the plate is held by a bolted joint.

REFERENCES

1. **Younis, N. T., (2005),** "Bolt Preload Effects on Stresses around Circular Holes" The 5th Jordanian International Mechanical Engineering Conference, Amman, Jordan.

2. **Chen. K. T., Ting. K. and Yang. W. S., (2000),** "Analysis of Stress Concentration Due to Irregular Ligaments in an Infinite Domain Containing a Row of Circular Holes" Mech. Struct & Mach. 28, 65-84.

3. **Ting, K., Chen, K. T. and Yang, W. S., (1999),** "Applied Alternating Method to Analyze the Stress Concentration around Interacting Multiple Circular Holes in an Infinite Domain", International Journal of Solids and Structures 36, 533-556.

4. **Meguid, S. A. and Gong, S. X., (2003)**, "Stress Concentration around Interacting Circular Holes: A Comparison between Theory and Experiments", Engineering Fracture Mechanics 44, 247-256.

5. **Younis, N. T., (2006),** "Assembly Stress for the Reduction of Stress Concentration" Mechanics Research Communications 33, 837-845.

6. **Guo, S. J., (2007),** "Stress Concentration and Buckling Behavior of Shear Loaded Composite Panels with Reinforced Cutouts", Composite Structures 80, 1-9.

7. **Liqing, W. and Bingzheng, G., (2008),** "Numerical Computation of Stress Intensity Factors for Bolt-hole Corner Crack in Mechanical Joints", Chinese Journal of Aeronautics 21, 411-416.

8. **Grosse, I. R. and Mitchell, L. D., (1990),** "Nonlinear Axial Stiffness Characteristics of Axisymmetric Bolted Joints", ASME Journal of Mechanical Design 12, 442-449.

9. **Lehnhoff, T. F., Ko, K. and McKay, M. L., (1994),** "Member Stiffness and Contact Pressure Distribution of Bolted Joints", Journal of Mechanical Design 16, 550-557.

10. **Lehnhoff, T. F. and Bunyard, B. A., (2000),** "Bolt Thread and Head Fillet Stress Concentration Factors", Journal of Pressure Vessel Technology 122, 180-185.

11. **Barrett, R. T., (2005),** "Stress Concentration Factors for Fasteners and Fastener Joints", American Fastener Journal 22, 60-61.

12. **Venkatesan, S. and Kinzel, G. L., (2006),** "Reduction of Stress Concentration in Bolt-Nut Connectors", Journal of Mechanical Design 128, 1337-1342.

13. **Turvey, G. J. and Wang, P., (2008),** "An FE Analysis of the Stresses in Pultruded GRP Single-Bolt Tension Joints and Their Implications for Joint Design", Computers and Structures 86, 1014-1021.

14. **Gao, F. and Kang. H., (2008),** "Effect of Pre-tensioned Rock Bolts on Stress Redistribution around a Roadway", Journal of China University of Mining and Technology 18, 509-515.

15. **Iyer, K., (2001),** "Solutions for Contact in Pinned Connections", Int. J. Solids Structure 38, 9133-9148.

16. **Li, R., Kelly, D., and Crosky, A., (2002),** "A Strength Improvement by Fiber Steering Around a Pin Loaded Hole", Composite Structure 57, 377-383.

17. **Okutan, B., (2002),** "The Effect of Geometric Parameters on the Failure Strength for Pin-loaded Multi-directional Fiber-glass Reinforced Epoxy Laminate", Composites 33, 567-578.

18. **McCarthy, C. T., McCarthy, M. A. and Lawlor, V. P., (2005),** "Progressive Damage Analysis of Multi-bolt Composite Joints with Variable Hole Clearance", Composites 36, 290-305.

19. **Yavari, V., Rajabi, I., Daneshavar, F. and Kadivar, M. H., (2009),** "On the Stress Distribution around the Hole in Mechanically Fastened Joints", Mechanics Research Communications 36, 373-380.

20. **Dally, J. W. and Riley, W. F., (1991),** Experimental Stress Analysis. McGraw Hill.

21. **Holman, J. P., (20001),** Experimental Methods for Engineers. McGraw Hill.

22. **Younis, N. T., (2003),** "Designing an Optical Force Transducer", Optical Engineering 42, 151-158.

23. **Younis, N. T., (2010),** "Visualized Photoelastic Images for Stress Concentration Instruction" The 2010 Annual ASEE Conference, Louisville, USA.